A Combined Plasmachemical and Emulsion Templating Approach for Actuated Macroporous Scaffolds

*Suzanne Morsch, Thomas J. Wood, Wayne C. E. Schofield, and Jas Pal S. Badyal**

Functionalised macroporous scaffolds have been fabricated by a decoupled two-step approach comprising plasmachemical deposition of the host material followed by spontaneous emulsion formation using templating molecules. This unique approach allows pore architecture and surface functionalisation to be tailored independently. Other key features encompass conformality to a range of substrate materials or geometries, and the scope for introduction of a wide variety of pore surface functionalities, which for instance include pore size actuation.

1. Introduction

Materials containing interconnected pores are important to a plethora of applications including gas storage,[1,2] fuel cells,[3] catalysis,[4,5] sensors,[6] filtration,[7] chromatography,[8,9] tissue engineering,[10,11] microfluidic devices,[12,13] and biomineralization.[14] Polymeric scaffolds are particularly attractive for many of these cases due to their low cost and light weight. The most common approach for making porous polymer structures involves templated polymerization around the aqueous phase of water in oil emulsions (polyHIPEs). Variants of this methodology include templated polymerization around alternative porogenic substances such as salt crystals,[15] colloids,[16] and non-solvents,[17] where the final macroporous structures are obtained by drying, etching, or leaching for porogen extraction. There are drawbacks in all of these cases which include large consumption of organic solvents and reagents, as well as waste disposal. Moreover, polyHIPE materials are renowned for their poor mechanical properties,[18–20] making them difficult to implement for many applications (such as catalysis, fuel cells, microfluidics, tissue engineering), where in fact thin macroporous films supported on a robust substrate would be a more viable alternative. One approach employed in the past to produce supported polyHIPE films has been the "breath figure method" whereby the condensation of water droplets onto a spin cast polymer layer serves to template an interconnected pore structure.[21] Nonetheless, even in this instance, there are inherent disadvantages including the prerequisite for precisely controlled humidity and a need for organic solvents (the evaporation of which drives water condensation). Furthermore, such spin casting often presents poor adhesion to the underlying substrate.

In this article, a plasmachemical deposition approach combined with molecule templating is described that decouples pore functionalisation from pore formation. Furthermore, it minimises the usage of expensive reagents and waste generation, as well as offering applicability to a whole host of substrate materials and geometries.[22] Firstly, structurally well-defined functional layers are produced by introducing the film precursor into a pulsed electrical discharge.[23,24] Mechanistically, this entails the generation of active sites in the gas phase and also at the growing film surface during the short duty cycle on-period (microseconds) followed by conventional polymerization mechanisms proceeding throughout the prolonged duty cycle off-period (milliseconds) in the absence of any UV-, ion-, or electron-induced damage.[25,26] The inherent reactive nature of the electrical discharge ensures good adhesion to the underlying substrate via free radical sites created at the interface during ignition of the plasma. Previous examples of pulsed plasma deposited well-defined functional films include poly(glycidyl methacrylate),[27,28] poly(bromoethyl-acrylate),[29] poly(vinyl aniline),[30] poly(vinylbenzyl chloride),[31] poly(allylmercaptan),[32] poly(*N*-acryloylsarcosine methyl ester),[33] poly(4-vinyl pyridine),[34] and poly(hydroxyethyl methacrylate).[35]

Although plasmachemical functionalisation of preassembled porous supports is well known,[36] the only attempts to directly induce porosity into plasma deposited films have entailed selective leaching of low molecular weight material[37] which has suffered from a lack of control over length scales and blistering or dissolution.[38] In this study, we demonstrate that plasmachemical deposited functional layers can be templated to yield macroporous films containing an interconnected open cell structure by introducing amphiphilic mediating species (such as cresyl violet perchlorate or sodium dodecyl sulphate) in combination with a non-solvent (such as water). Furthermore, the host plasma polymer functional groups provide scope for secondary functionalisation of the generated macroporous structure. For instance, poly(vinylbenzyl chloride) films can be utilised for surface initiated atom transfer radical polymerization (ATRP) of poly(glycidyl methacrylate) to yield epoxide polymer brush functionalised macroporous layers, **Scheme 1**. These can then be employed as scaffolds for actuated control of porosity.

S. Morsch, T. J. Wood, Dr. W. C. E. Schofield, Prof. J. P. S. Badyal
Department of Chemistry
Science Laboratories
Durham University
Durham DH1 3LE, England, UK
E-mail: j.p.badyal@durham.ac.uk

DOI: 10.1002/adfm.201102020

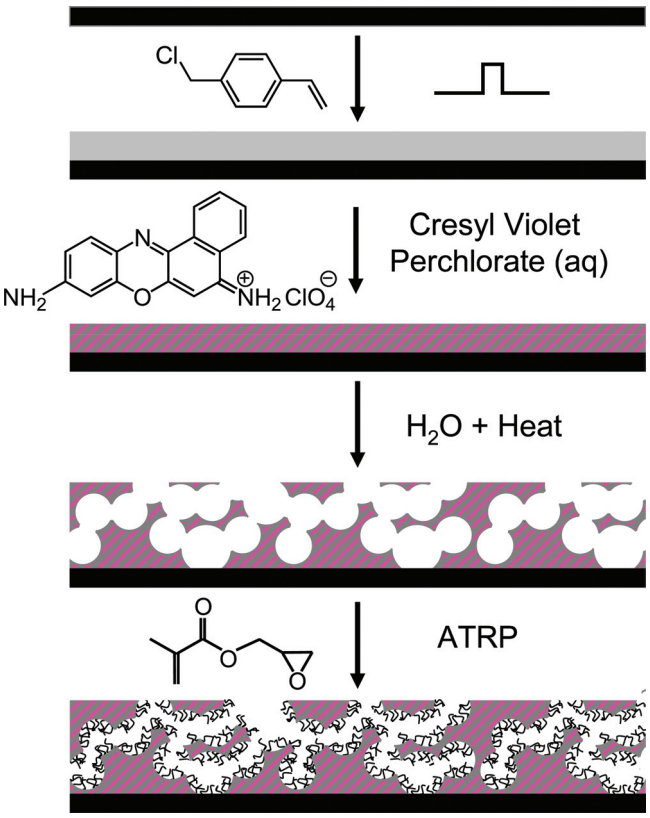

Scheme 1. Formation of porous pulsed plasma deposited poly(vinylbenzyl chloride) films by immersion in cresyl violet perchlorate solution followed by rinsing in water at elevated temperature, and then additional surface functionalisation of pores (e.g., ATRP).

2. Results

2.1. Pulsed Plasma Deposition of Poly(vinylbenzyl chloride)

XPS analysis of pulsed plasma deposited poly(vinylbenzyl chloride) yielded elemental compositions corresponding to the expected theoretical values based on the vinylbenzyl chloride precursor, thereby indicating good structural retention of the benzyl chloride functionality,[31] Structure 1 (**Scheme 2**) and **Table 1**. In addition, the absence of a Si(2p) X-ray photoelectron spectroscopy (XPS) signal confirmed pinhole-free coverage of the underlying silicon wafer substrate.

Further evidence for the structural integrity of pulsed plasma deposited poly(vinylbenzyl chloride) films was obtained by

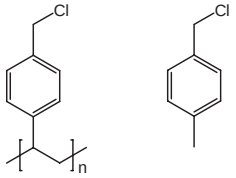

Scheme 2. Structures **1** and **2**.

Table 1. XPS elemental compositions of pulsed plasma deposited poly(vinylbenzyl chloride).

Pulsed Plasma Deposited Poly(vinylbenzyl chloride)		Elemental Composition			
		C%	O%	N%	Cl%
As deposited	Theoretical	90	0	0	10
	Experimental	90 ± 1	0	0	10 ± 1
Immersion in cresyl violet (aq)	Experimental	73 ± 2	20 ± 2	4 ± 1	3 ± 1
Cresyl violet (aq) + 16 h water rinsing at 22 °C	Experimental	79 ± 2	14 ± 2	2 ± 1	5 ± 1

infrared spectroscopy, where the main fingerprint features matched those associated with the monomer, **Figure 1**. These include halide functionality at 1263 cm^{-1} (CH_2 wag mode

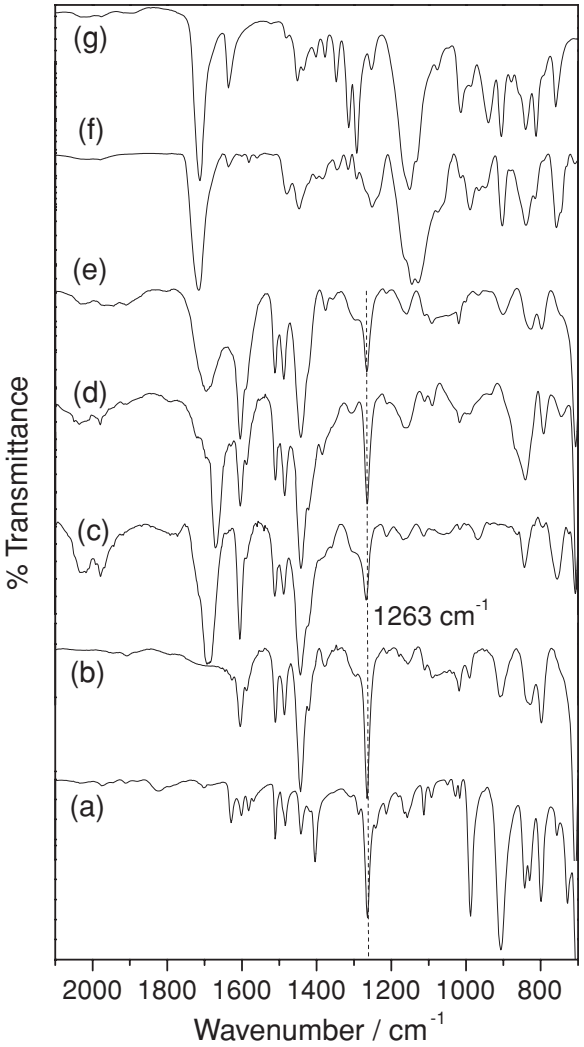

Figure 1. Infrared spectra of: a) vinylbenzyl chloride monomer; b) pulsed plasma deposited poly(vinylbenzyl chloride); c) pulsed plasma deposited poly(vinylbenzyl chloride) following immersion in cresyl violet perchlorate solution; d) following 16 h water rinsing of (c) at 22 °C and drying for 16 h in air at 22 °C; e) following immersion of (d) in water at 60 °C for 1 hr and then drying for 16 h in air at 22 °C; f) poly(glycidyl methacrylate) ATRP grafted onto (e); and (g) glycidyl methacrylate monomer.

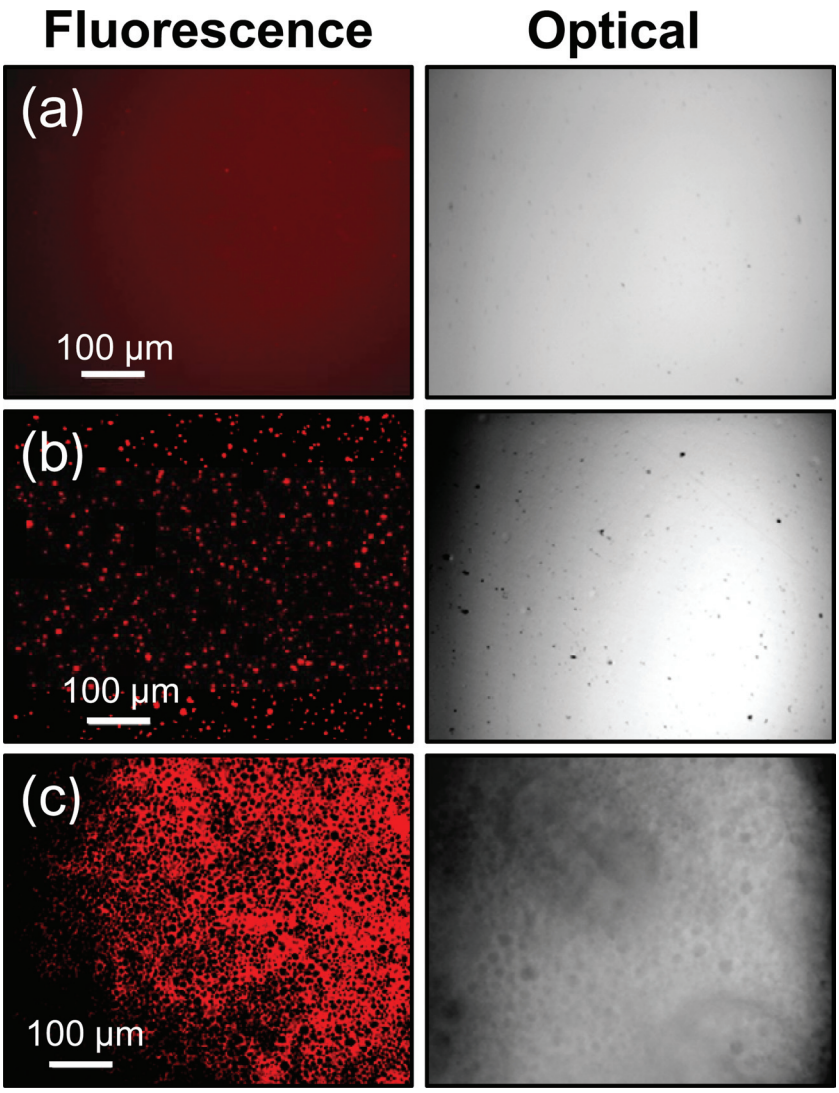

Figure 2. Fluorescence and corresponding optical micrographs (×10 magnification) of pulsed plasma deposited poly(vinylbenzyl chloride) films: a) as deposited; b) following immersion in cresyl violet solution; and c) following immersion in cresyl violet perchlorate solution, rinsing in water at 22 °C for 16 h, soaking in water at 60 °C for 60 min, and then drying in air at 22 °C for 16 h.

for CH_2–Cl) and para-substituted benzene ring stretches at 1495 cm^{-1} and 1603 cm^{-1}.[39] In addition, disappearance of the vinyl double bond stretch at 1629 cm^{-1} is consistent with polymerization.

A linear film deposition rate of 191 ± 17 nm min^{-1} and water contact angle values of 80 ± 1° (not hydrophilic) were measured. Optical micrographs and fluorescence images (gathered at the excitation wavelength for cresyl violet perchlorate) were both featureless, thereby confirming that the deposited films were smooth and homogenous, **Figure 2**.

2.2. Interaction with Cresyl Violet Perchlorate Amphiphile

Fluorescence microscopy showed that immersion of pulsed plasma deposited poly(vinylbenzyl chloride) films in cresyl violet perchlorate solution for 16 h resulted in uptake of the fluorophore, Figure 2. Subsurface penetration of cresyl violet perchlorate was evident by the greater number of crystals detected by fluorescence microscopy compared to those visible at the surface by optical microscopy, Figure 2. Furthermore, XPS elemental analysis confirmed the presence of cresyl violet perchlorate on the surface of pulsed plasma deposited layers via detection of N(1s) and O(1s) fluorophore signals, Table 1. Infrared spectroscopy identified a broad absorbance centred at 1690 cm^{-1} (H–O–H bend attributed to the crystallisation of water associated with cresyl violet perchlorate),[39,40] Figure 1. This was found to be absent when *N,N*-dimethylformamide was employed instead as the solvent for cresyl violet perchlorate under otherwise identical conditions (*N,N*-dimethylformamide is an alternative polar solvent that dissolves cresyl violet perchlorate).[41] Retention of the benzyl chloride infrared absorbances confirmed that no chemical changes to the polymer bulk had taken place during contact with aqueous cresyl violet perchlorate solution, Figure 1.

In addition to the aforementioned macroscale examination by fluorescence and optical microscopy, atomic force microscopy (AFM) was employed to monitor the microscale structure. Tapping-mode height images confirmed that pulsed plasma deposited poly(vinylbenzyl chloride) surfaces were featureless, and only a slight roughening was visible following 16 h immersion in high purity water and then drying in air at 22 °C for 16 h, **Figure 3**. In contrast, immersion in aqueous cresyl violet perchlorate solution for 16 h and then drying in air at 22 °C for 16 h gave rise to crater formation around crystals on the film surface. Subsequent rinsing of these samples in high-purity water at room temperature for 16 h removed the crystals to yield additional crater features. Partial removal of cresyl violet perchlorate from the surface during rinsing is supported by XPS analysis, which indicated a corresponding drop in surface oxygen and nitrogen content associated with the fluorophore, Table 1 and Scheme 1.

Interactions between cresyl violet perchlorate and the pulsed plasma deposited poly(vinylbenzyl chloride) films was further investigated using 4-methylbenzyl chloride as an analogue to represent the pendant benzyl chloride functionality contained in the pulsed plasma deposited layers; Structures 1 and 2 in Scheme 2. Infrared spectra taken for 1 g dm^{-3} solutions of cresyl violet perchlorate in 4-methylbenzyl chloride showed no perturbation in the position or intensity of the fingerprint region infrared absorbances for 4-methylbenzyl chloride, thereby providing further confirmation that no chemical reaction is to be expected to occur between the pulsed plasma deposited poly(vinylbenzyl chloride) layers and cresyl violet

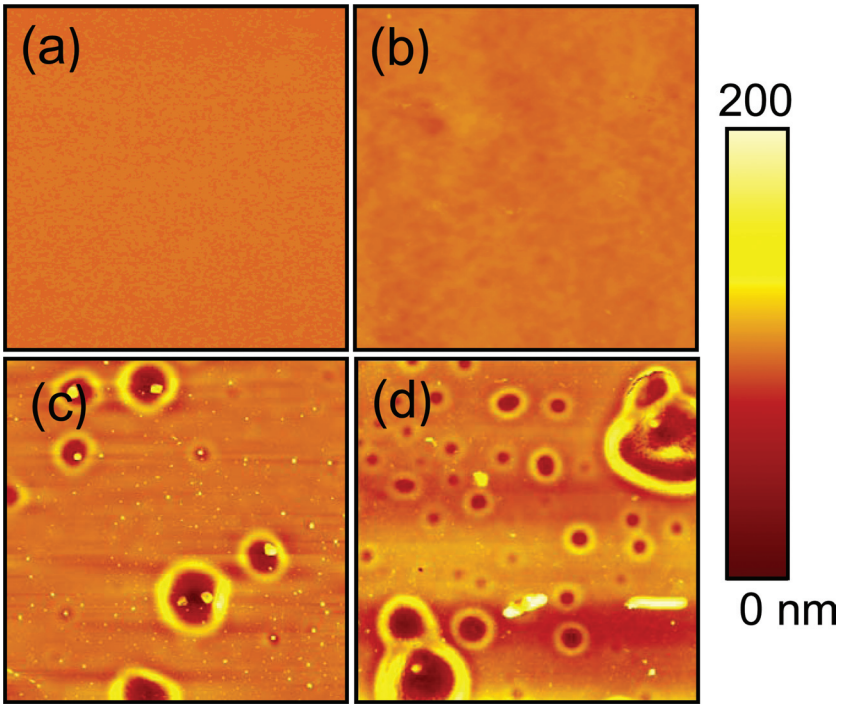

Figure 3. 20 μm × 20 μm AFM microscopy images of pulsed plasma deposited poly(vinylbenzyl chloride) surfaces: a) as deposited; b) following rinsing in high purity water for 16 h and then drying in air at 22 °C for 16 h; c) following 16 h immersion in aqueous cresyl violet perchlorate solution; and d) following rinsing of (c) in high purity water for 16 h and then drying in air at 22 °C for 16 h.

perchlorate, **Figure 4**. Moreover, subtraction of the 4-methylbenzyl chloride infrared spectrum from that of the solution yielded the characteristic absorbances of cresyl violet perchlorate. These absorbances were comparable in width to those measured for cresyl violet perchlorate dissolved in water, and notably sharper than those observed for the bulk crystalline material, **Table 2**. This is indicative of free rotation in both liquids, i.e., cresyl violet perchlorate can be solvated by both water and 4-methylbenzyl chloride (and therefore poly(vinylbenzyl chloride)).

2.3. Macroporous (polyHIPE) Structure Formation

In order to create macropores, the aforementioned samples (which had been immersed in aqueous cresyl violet perchlorate solution and rinsed in water) were stored in high purity water for 1 h at 60 °C. During this period, the polymer layer appearance changed from translucent (prior to heating) to opaque, and remained so upon subsequent drying in air. Fluorescence and optical micrographs revealed an interconnected polyHIPE structure (pore diameters of 1–10 μm) which is comparable to the 3D pore geometry of conventional polyHIPE structures,[43,44] Figure 2. These macropores were clearly visible by high-resolution scanning electron microscopy (SEM), **Figure 5**. Moreover, the smooth and largely spherical pore morphology is consistent with solvent templating.[45–47] Cross-sectional SEM microcopy images confirm that porosity extends throughout the polymer films, which are distended from an initial thickness of 3 μm to 10 μm. These measurements effectively eliminate partial dissolution of plasmachemical polymer layers as being an alternative explanation for the creation of pores.[37]

A series of control experiments using alternative reagents were undertaken to further elucidate the mechanism of pore formation. These employed identical conditions to those already used to generate the macroporous structures in pulsed plasma deposited poly(vinylbenzyl chloride) films (i.e., 16 h immersion in dissolved cresyl violet perchlorate solution, 16 h rinsing in solvent at 22 °C, immersion in solvent at 60 °C for 1 h, and air drying). First of all, rinsing the pulsed plasma deposited poly(vinylbenzyl chloride) films with only deionised water (in the absence of cresyl violet perchlorate) produced no porosity (featureless AFM, fluorescence and optical microscopy images), thereby confirming that cresyl violet perchlorate plays a critical role in pore formation. Replacement of water with *N,N,*-dimethylformamide (an alternative polar solvent) throughout also resulted in the absence of porosity, which demonstrates the importance of water for templating. Finally, the choice of sodium dodecyl sulphate as a different amphiphile to cresyl violet perchlorate for mediating the interaction between water and pulsed plasma deposited poly(vinylbenzyl chloride) films (16 h immersion in 0.5% (w/v) aqueous sodium dodecyl sulphate solution, followed by rinsing in water, heating at 60 °C in water, and drying) caused the appearance of the polymer film to change from translucent to opaque during heating, and SEM images taken after drying revealed the formation of macroporous (polyHIPE) structures, thereby confirming that amphiphilic surfactant action between water and pulsed plasma deposited poly(vinylbenzyl chloride) underpins the formation of macroporous structures, **Figure 6**.

2.4. Surface Functionalisation of Macropores

Pulsed plasma deposited poly(vinylbenzyl chloride) layers have previously been used for the initiation of atom transfer radical polymerization (ATRP) to create polymer brushes.[31,33] The infrared spectra of the fabricated porous poly(vinylbenzyl chloride) films indicated retention of the ATRP initiating benzyl chloride functionality, Figure 1. Therefore ATRP grafting of glycidyl methacrylate onto the macroporous films was undertaken, and infrared spectroscopy showed characteristic signature absorbances of poly(glycidyl methacrylate)[27,39] at 1726 cm^{-1} (C=O ester stretch, instead of 1714 cm^{-1} for the monomer due to conjugation with the vinyl group), 1152 cm^{-1} (C–O stretch), 1254 cm^{-1} (epoxide ring breathing), 906 cm^{-1} (antisymmetric epoxide ring

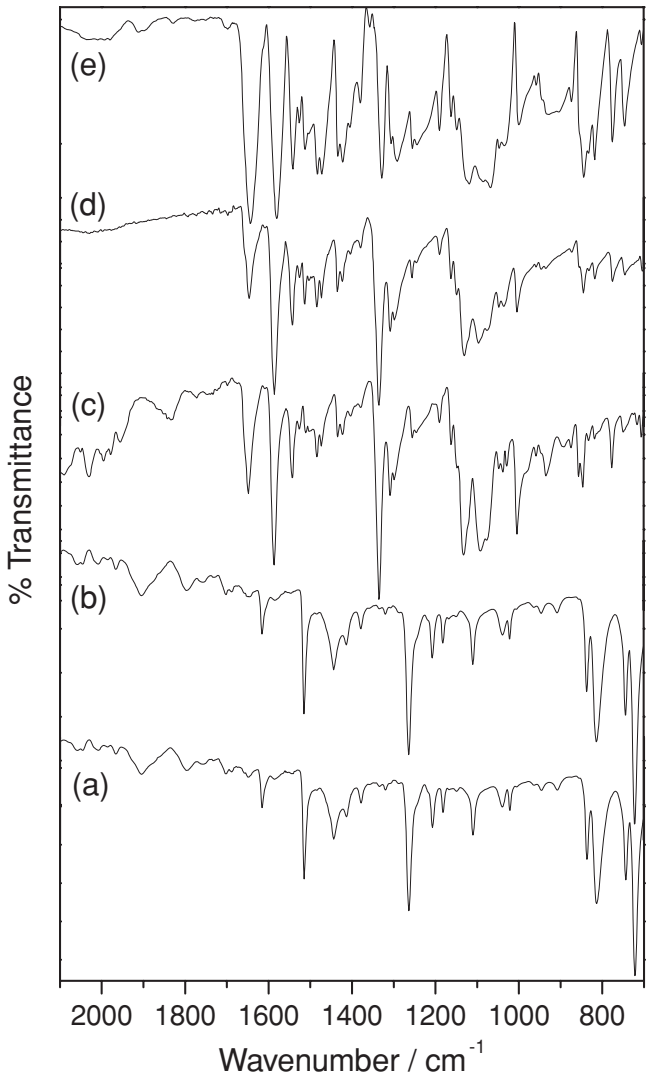

Figure 4. Infrared spectra of: a) 4-methylbenzyl chloride; b) 0.1 mg dm^{-3} solution of cresyl violet perchlorate in 4-methylbenzyl chloride; c) solvent subtracted spectrum of cresyl violet perchlorate dissolved in 4-methylbenzyl chloride; d) solvent subtracted spectrum cresyl violet perchlorate dissolved in water; and e) cresyl violet perchlorate bulk crystalline material.

deformation), and 841 cm^{-1} (symmetrical epoxide ring deformation), Figure 1. Absence of the glycidyl methacrylate monomer vinyl absorbances at 1637 cm^{-1} (C=C stretch) and 941 cm^{-1} (vinyl CH_2 wag) provided additional evidence for ATRP having taken place.

Table 2. Infrared full-width-at-half-maximum (FHWM) peak widths corresponding to Figure 4.

Absorbance[42]	Peak FWHM [cm^{-1}]		
	4-Methylbenzyl chloride Solution	Water Solution	Bulk Crystal
1642 cm^{-1} (in plane fused ring vibration)	20	23	36
1579 cm^{-1} (NH bending of amino groups)	15	18	26
1543 cm^{-1} (NH_2 out-of-plane bend)	10	11	17

Subsequent fluorescent tagging of the poly(glycidyl methacrylate) brushes via nucleophilic ring opening of the epoxide centres was carried out using a dilute solution of Alexafluor 350 Cadaverine dye, **Scheme 3**. Fluorescence microscopy confirmed the reaction of the fluorophore with the poly(glycidyl methacrylate) brushes, **Figure 7**. Imaging at the excitation wavelengths of 640 nm and 360 nm for both cresyl violet perchlorate and Alexafluor 350 Cadaverine dye respectively confirmed the grafting of poly(glycidyl methacrylate) brushes directly onto the underlying porous structure, Figure 7.

2.5. Pore-Size Actuation

ATRP grafted poly(glycidyl methacrylate) brushes tagged with Alexafluor 350 Cadaverine dye have previously been shown to exhibit solvent-responsive behaviour.[48] Owing to the hydrophilic nature of the fluorophore, these tagged brushes swell upon exposure to water, which in turn can be removed by exposure to hygroscopic organic solvents. The thickness (length) of the ATRP grafted poly(glycidyl methacrylate) brushes[48] was optimised so as to be comparable in dimension to the host pore sizes when extended (swollen). AFM topography measurements of such ATRP grafting of poly(glycidyl methacrylate) onto macroporous poly(vinylbenzyl chloride), followed by reaction with Alexafluor 350 Cadaverine dye and extensive aqueous rinsing, showed complete coverage of pore features, thereby indicating that the swollen tagged poly(glycidyl methacrylate) brushes have filled the pores, **Figure 8**. Furthermore, the underlying porous poly(vinylbenzyl chloride) structure could be observed using fluorescence microscopy taken at the excitation wavelength for cresyl violet perchlorate (640 nm - red), whilst those taken using the excitation wavelength of Alexafluor 350 Cadaverine dye (360 nm - blue) over the same area showed very little contrast, indicating the presence of the tagged polymer brushes across the entire pore structure. Water removal from these layers was accomplished by soaking in a hygroscopic solvent (tetrahydrofuran), which resulted in the restoration of porosity, as verified by both by fluorescence microscopy and AFM height images, Figure 8. This behaviour (actuation) was found to be reversible.

3. Discussion

Macroporous polymers are ordinarily fabricated using high internal phase emulsion (HIPE) techniques, where the continuous organic phase consists of the monomer templated around the internal aqueous phase prior to polymerization, and then the aqueous phase is removed to leave behind a micron-scale interconnected porous structure.[49] These emulsions are necessarily stabilised by the addition of surfactants (which serve to lower the interfacial energy between the two phases, and hence prevent separation), but nonetheless their formation involves extensive mixing of the organic and aqueous phases. In marked contrast, the present study has demonstrated a completely different approach, where polymerization takes place

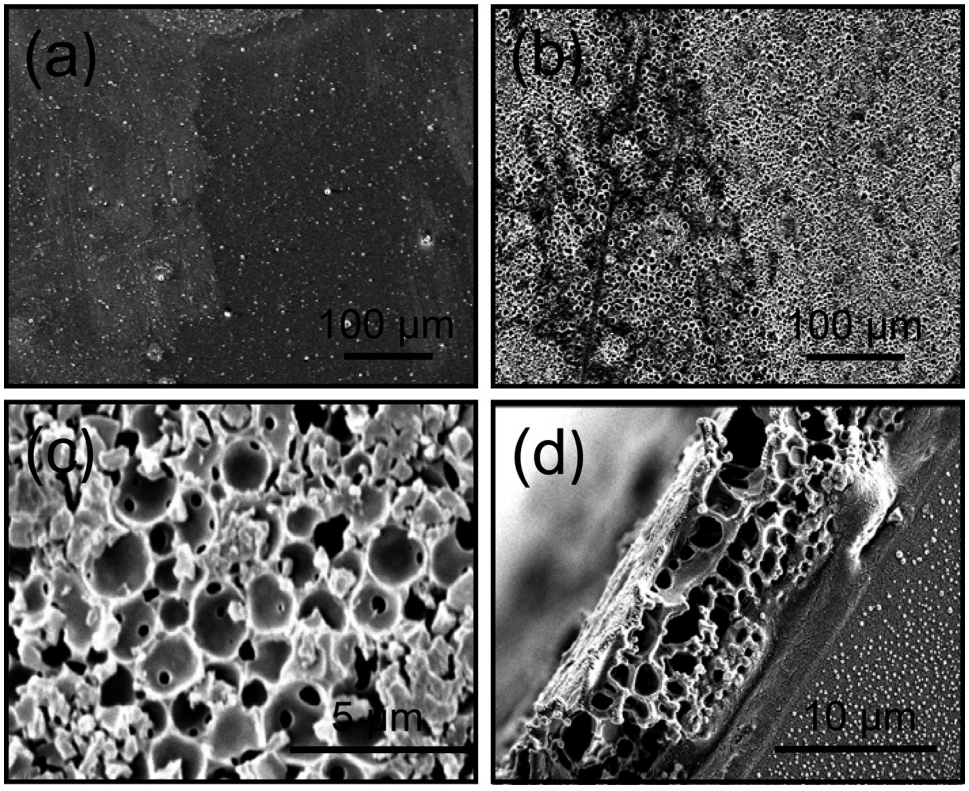

Figure 5. SEM images of pulsed plasma deposited poly(vinylbenzyl chloride) following 16 h immersion in aqueous cresyl violet perchlorate solution and then: a) subsequent immersion in water at 22 °C for 1 h and drying in air at 22 °C for 16 h; b–d) subsequent immersion in water at 60 °C for 1 h and drying in air at 22 °C for 16 h, where (d) corresponds to the cross-section. The pore diameters range between 1–10 μm. The interconnecting pore hole size range is 201 ± 65 nm in diameter. The pore wall thickness range is 172 ± 80 nm.

prior to pore formation. At elevated temperatures spontaneous emulsion formation occurs between the pulsed plasma deposited polymer (impregnated with amphiphilic species) and water to create macroporous structures. This is consistent with spontaneous microemulsion formation where a mediating

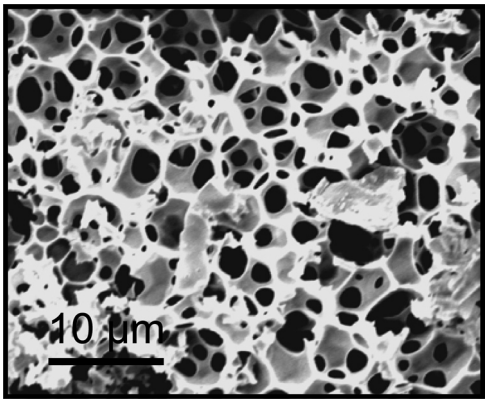

Figure 6. SEM image of pulsed plasma deposited poly(vinylbenzyl chloride) following immersion in aqueous sodium dodecyl sulphate solution at 22 °C, then immersion in water at 60 °C for 1 h, and finally drying in air at 22 °C for 16 h.

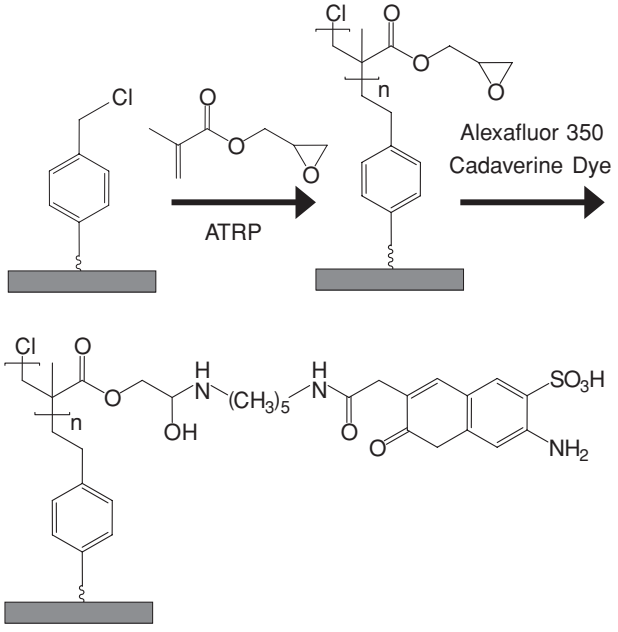

Scheme 3. ATRP grafting of glycidyl methacrylate onto pulsed plasma deposited poly(vinylbenzyl chloride) initiator layer followed by nucleophilic ring opening of the epoxide centres by Alexafluor 350 Cadaverine dye.

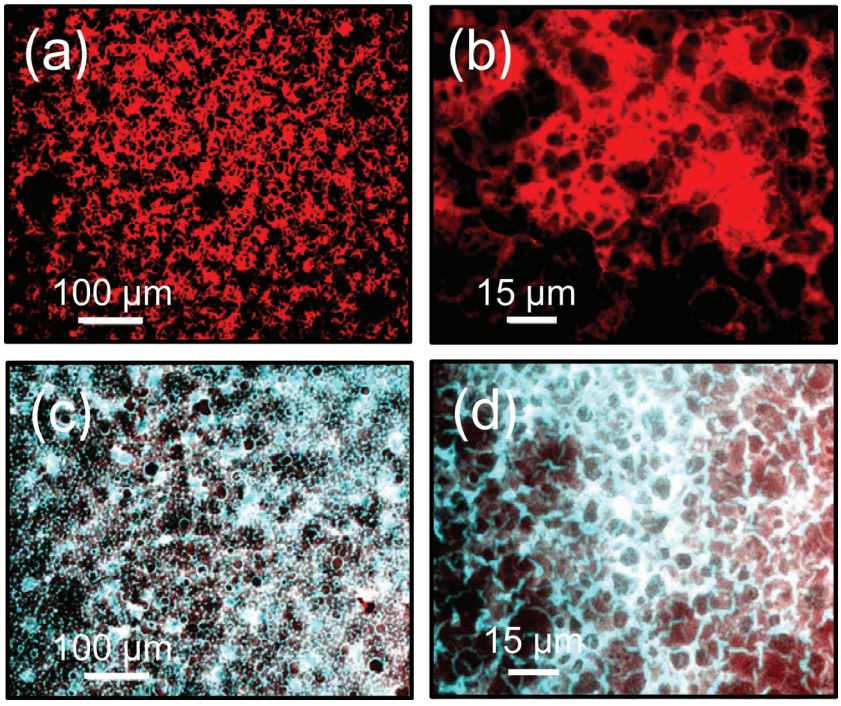

Figure 7. Fluorescence microscopy images of pulsed plasma deposited poly(vinylbenzyl chloride): a,b) following immersion in aqueous cresyl violet perchlorate solution for 16 h, and then rinsing in water at 60 °C for 1 h (red excitation at 640 nm for cresyl violet perchlorate); and c,d) following exposure of (a) and (b) to ATRP grafting conditions for glycidyl methacrylate for 4 hr and then immersion in Alexafluor 350 Cadaverine dye (excitation wavelengths for cresyl violet perchlorate (640 nm - red) and Alexaflour 350 Cadaverine dye (360 nm - blue)).

(surfactant) species lowers interfacial energy between two immiscible phases to such an extent that the contacting area is spontaneously maximised by emulsion formation.[50,51] In the present case of cresyl violet perchlorate, favourable interaction with both water and pulsed plasma deposited poly(vinylbenzyl chloride) can be understood by consideration of its molecular structure, Scheme 1. The ionic component of the molecule confers hydrophilicity, whilst the extended aromatic structure facilitates interaction with the benzyl chloride moieties contained within the pulsed plasma deposited poly(vinylbenzyl chloride) film. Control experiments using 4-methylbenzyl chloride has confirmed this behaviour, Figure 4. Indeed, many similar organic dyes have previously been shown to disperse within aromatic polymer matrices via π–π interactions.[52,53] The utilization of an alternative amphiphilic species (sodium dodecyl sulphate, which is known to mediate interactions between vinylbenzyl chloride and water[54,55]) has also been shown to impart porosity. In contrast, organic solvents (such as *N,N,*-dimethylformamide) are less expected to form emulsions with polymers due to their higher miscibility.[56] Indeed, poly(vinylbenzyl chloride) has been reported to dissolve in *N,N,*-dimethylformamide,[57] which helps to account for why the pulsed plasma deposited poly(vinylbenzyl chloride) layers are not templated by *N,N,*-dimethylformamide solutions.

In keeping with conventional bulk emulsion polymerization methods, a finite amount of the surfactant is retained.[58] This is due to the equilibrium dispersion of surfactant between organic and aqueous phases. UV–vis measurements showed that cresyl violet perchlorate partially disperses from aqueous solutions into 4-methylbenzyl chloride liquid, and vice versa following a 16 h equilibration period. In the present study, the retention of a very small amount of cresyl violet perchlorate fluorophore within the porous polymer films has allowed fluorescence microscopy to be used as a tool, which offers the advantage of film inspection under ambient conditions (in contrast to SEM) as well as examination of subsurface morphology.

Apart from the mediating effect of surfactants, the stability of conventional water in oil microemulsions can also be enhanced by increasing the viscosity of the organic phase.[59] For the case of pulsed plasma deposited poly(vinylbenzyl chloride), although these films are not sufficiently flexible at room temperature to form emulsions, the plasmachemical layer can be considered to become a highly viscous organic phase at elevated temperatures. AFM height images show shallow crater formation at the film surface following exposure to cresyl violet perchlorate solution under ambient conditions, which is indicative of a limited amount of film deformation occurring at the solid/liquid interface around water droplets in order to maximise interfacial contact, Figure 3. This effect is enhanced at raised temperatures, with the greater polymer chain mobility allowing them to stretch around water droplets to create an emulsion. This is akin to the thermoplastic behaviour of conventional poly(vinylbenzyl chloride), which becomes more flexible at elevated temperatures.[60,61]

The proposed mechanism for pore generation is therefore dependent upon a combination of surfactant action and polymer flexibility. A key feature is that unlike traditional approaches where polymerization takes place post emulsion (pore) formation, the present method effectively decouples the polymerization step completely from emulsion formation. This is important given that conventional emulsions used to fabricate polyHIPE materials are highly complex formulations comprising solvents, surfactants, monomer(s), cross-linker, and polymerization initiators, where the molecular structure and concentration of each of these components affects emulsion stability and the resulting pore dimensions and morphology.[49,62] In such cases, porosity is also influenced by further factors including the material of the container contacting the emulsion during polymerization, temperature, and mixing speed.[49] Overall this means that a delicate balance of process conditions is required to reproducibly fabricate conventional open cell macroporous polymers. By decoupling the polymerization step, the present method allows for better control over the macromolecular architecture for a variety of surfactants (including cresyl violet perchlorate, which is not ordinarily considered to behave as a surfactant due to its small size). Raising the temperature can be expected to affect the flexibility of the pulsed plasma deposited poly(vinylbenzyl

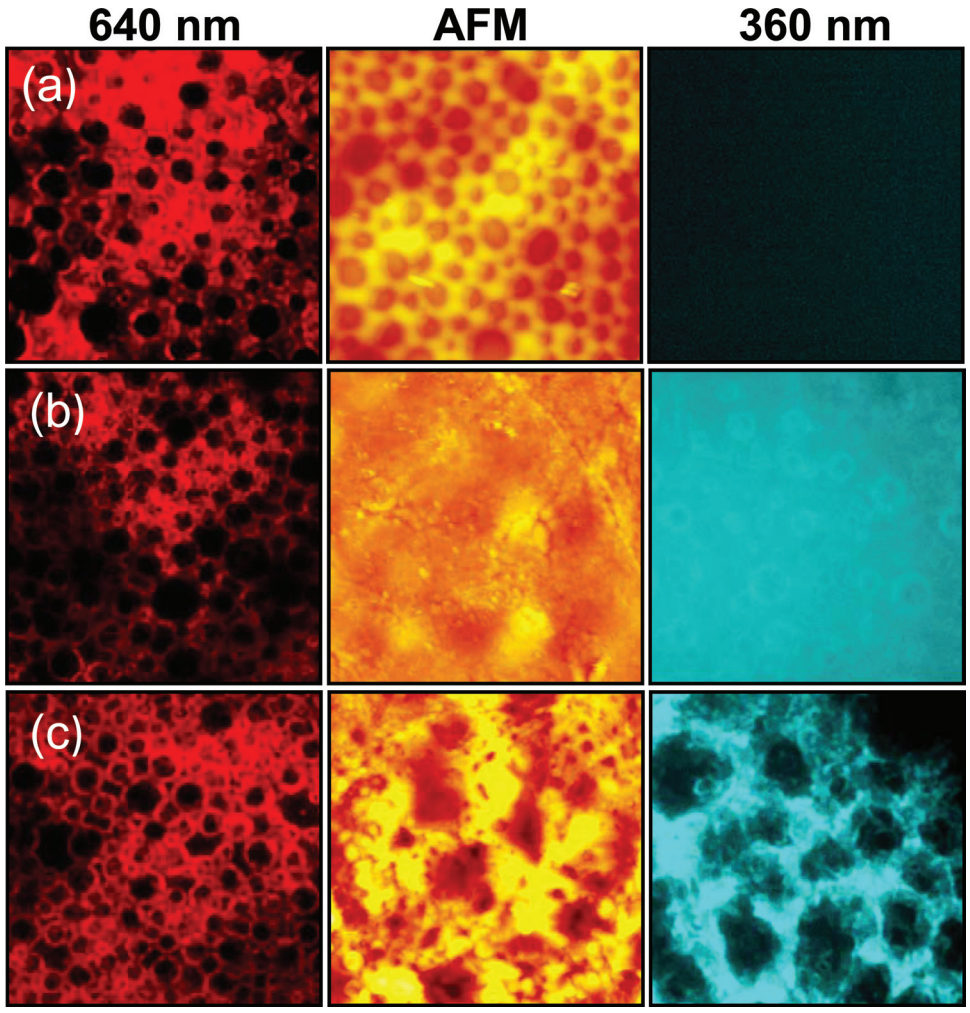

Figure 8. 50 µm × 50 µm tapping-mode AFM images (z scale is 1500 nm) and corresponding fluorescence micrographs (excitation wavelengths for cresyl violet perchlorate (640 nm - red) and Alexafluor 350 Cadaverine dye (360 nm - blue)) of pulsed plasma deposited poly(vinylbenzyl chloride): a) following immersion in aqueous cresyl violet perchlorate solution, and then rinsing at 60 °C for 1 h; b) following exposure of (a) to ATRP grafting conditions for glycidyl methacrylate for 12 h, brief immersion in Alexafluor 350 Cadaverine dye, followed by 16 h aqueous rinsing at 22 °C; and c) following immersion of (b) in tetrahydrofuran and drying.

chloride) layer during the pore formation step, which will lead to increased coalescence of water phase droplets to yield larger pore sizes (analogous to decreased viscosity of the organic phase of a standard HIPE mixture[60,61,63]). Other variables for controlling pore size include pressure[64] and surfactant concentration.[65] Furthermore, given that the flexibility of the pulsed plasma deposited poly(vinylbenzyl chloride) layers can be controlled by varying the plasma deposition parameters, this also provide a means for tailoring pore geometries. The main practical advantages of the described technique are that the plasmachemical deposition step is substrate-independent and solventless, whilst the spontaneous emulsion formation requires only the use of environmentally friendly aqueous solutions. A straightforward extension of this approach can be envisaged for the fabrication of a whole host of functionalised macroporous structures, given the wide range of well-defined plasmachemical deposited functional layers that are available. In addition, the generated macroporous structures can be further functionalised by either plasmachemical or conventional wet techniques (e.g., ATRP), which broadens the scope for potential applications (given the wide array of monomers and functionalities available - including bioactive hydrophilic polymers[66,67]).

4. Conclusions

Macroporous (polyHIPE) structures can be fabricated by impregnation of plasmachemical deposited polymeric films with an amphiphilic templating species followed by spontaneous emulsion formation. This enables the decoupling of pore functionalisation from pore formation. For instance, subsequent atom transfer radical polymerization (ATRP) of polymer brushes onto the pore surfaces facilitates pore size actuation. These

functionalised macroporous scaffold structures have potential application for catalysis, fuel cells, gas storage, and biotechnology.

5. Experimental Section

Pulsed Plasma Deposition of Poly(vinylbenzyl chloride): Plasma depositions were performed inside a cylindrical glass reactor (5.5 cm diameter, 475 cm^3 volume) located within a Faraday cage. The system was evacuated using a 30 L min^{-1} mechanical rotary pump via a liquid nitrogen cold trap (base pressure less than 3×10^{-3} mbar and leak rate better than 6×10^{-9} molecules per second[68]). A copper coil wound around the reactor (4 mm diameter, 10 turns, located 10 cm away from the gas inlet) was connected to a 13.56 MHz radio frequency (RF) power supply via an L-C matching network. The RF power supply was triggered using a signal generator. All apparatus was thoroughly scrubbed with detergent and hot water, rinsed with propan-2-ol, and oven dried. Substrate preparation comprised successive sonication of glass microscope slides (VWR International LLC) or silicon wafer (MEMC Electronic Materials Inc) in propan-2-ol and cyclohexane for 15 min each prior to insertion into the centre of the plasma reactor. Further cleaning entailed running a 50 W continuous wave air plasma at 0.2 mbar for 30 min. Vinylbenzyl chloride precursor (+97%, Aldrich) was loaded into a sealable glass tube, degassed via several freeze-pump-thaw cycles, and attached to the plasma deposition chamber. Monomer vapour was then allowed to purge through the apparatus at a pressure of 0.2 mbar for 3 min prior to electrical discharge ignition. Optimum pulsed plasma deposition duty cycle parameters were 100 μs on-period and 4 ms off-period in conjunction with 30 W peak power.[31] Following plasma extinction, precursor vapour was allowed to continue to pass through the system for a further 3 min, followed by evacuation to base pressure.

Porous Film Formation: Substrates bearing 3-μm-thick pulsed plasma-deposited poly(vinylbenzyl chloride) layers were immersed into 0.15 mg L^{-1} aqueous solution of cresyl violet perchlorate (analytical grade, Aldrich) for 16 h. Following removal from solution, the samples were thoroughly rinsed with high purity water (BS 3978 Grade 1), and soaked in fresh high-purity water for an additional 16 h at room temperature. In order to induce pore formation, the samples were then placed inside a sealed jar containing high purity water and stored at 60 °C for 1 h. Finally, the films were dried under ambient conditions for 16 h prior to analysis.

Surface Initiated ATRP of Poly(glycidyl methacrylate): Porous poly(vinylbenzyl chloride) functionalised substrates were placed inside a sealable glass tube containing copper(I) bromide (5 mmol, +98%, Aldrich), copper(II) bromide (1 mmol, +99%, Aldrich), 2,2'-bipyridyl (12 mmol, +99.9%, Aldrich), glycidyl methacrylate (0.05 mol, +97%, Aldrich), and propan-2-ol (4 mL, reagent grade, Fisher), Scheme 3. The mixture was thoroughly degassed using freeze-pump-thaw cycles and then allowed to undergo polymerization at room temperature for 4 h. Cleaning and removal of any physisorbed ATRP polymer was accomplished by successive rinsing with propan-2-ol and tetrahydrofuran. Fluorescent tagging of the surface grafted poly(glycidyl methacrylate) epoxide centers was achieved by brief submersion into a 1 mg dm^{-3} aqueous solution of Alexafluor 350 Cadaverine dye (analytical grade, Invitrogen Ltd), followed by extensive rinsing with high-purity water, Scheme 3.

Characterization: Film thicknesses following pulsed plasma deposition were measured using a spectrophotometer (nkd-6000, Aquila Instruments Ltd.). Transmittance-reflectance curves (350–1000 nm wavelength range) were aquired for each sample and fitted to a Cauchy material model using a modified Levenberg-Marquardt algorithm.[69]

Surface elemental compositions were obtained by X-ray photoelectron spectroscopy (XPS) using a VG ESCALAB II electron spectrometer equipped with a non-monochromated Mg Kα X-ray source (1253.6 eV) and a concentric hemispherical analyser. Photoemitted electrons were collected at a take-off angle of 20° from the substrate normal, with electron detection in the constant analyser energy mode (CAE, pass energy = 20 eV). Experimentally determined instrument sensitivity factors were taken as C(1s): N(1s): O(1s): Cl(2p) equals 1.00: 0.63: 0.39: 0.35.

Infrared spectra were acquired using a Fourier-transform infrared (FTIR) spectrometer (Perkin-Elmer Spectrum One) operating with a liquid nitrogen cooled MCT detector set at 4 cm^{-1} resolution across the 700–4000 cm^{-1} range. The instrument was fitted with a variable angle reflection-absorption accessory (Specac) set to an angle of 66° for silicon wafer substrates and adjusted for p-polarization.

Fluorescence microscopy was performed using an Olympus IX-70 system (DeltaVision RT, Applied Precision Inc, WA). Images were collected using excitation wavelengths of 640 nm and 360 nm corresponding to the absorption maxima of cresyl violet perchlorate and the Alexafluor 350 Cadaverine dye molecules, respectively.

Surface microscopy images were obtained with a scanning electron microscope (Cambridge Stereoscan 240). Prepared specimens were placed onto carbon discs and then mounted onto aluminium holders, followed by deposition of 15 nm gold coating (Polaron SEM coating unit). For cross-sectional images, samples were frozen and snapped under liquid nitrogen prior to mounting.

Atomic force microscopy (AFM) images were acquired in tapping mode at 20 °C in ambient air (Digital Instruments Nanoscope III, Santa Barbara, CA). The tapping mode tip had a spring constant of 42–83 Nm^{-1} (Nanoprobe Inc).

Sessile drop contact angle measurements were made at 20 °C using a video capture apparatus (VCA 2500 XE, AST Products Inc) and 2 μL high purity water droplets (BS 3978 Grade 1).

Acknowledgements

S.M. would like to thank UKIERI for financial support and T. Davey for assistance with SEM.

Received: August 25, 2011
Published online: November 10, 2011

[1] H. Furukawa, O. M. Yaghi, *J. Am. Chem. Soc.* **2009**, *131*, 8875.
[2] H. Wang, Q. Gao, J. Hu, *J. Am. Chem. Soc.* **2009**, *131*, 7016.
[3] Y. Ding, M. Chen, J. Erlebacher, *J. Am. Chem. Soc.* **2004**, *126*, 6876.
[4] J.-S. Yu, S. Kang, S. B. Yoon, G. Chai, *J. Am. Chem. Soc.* **2002**, *124*, 9382.
[5] S. J. Pierre, J. C. Thies, A. Dureault, N. R. Cameron, J. C. M. van Hest, N. Carette, T. Michon, R. Weberskirch, *Adv. Mater.* **2006**, *18*, 1822.
[6] C. Zhao, E. Danish, N. R. Cameron, R. Kataky, *J. Mater. Chem.* **2007**, *17*, 2446.
[7] Y. Ito, Y. Ochiai, Y. S. Park, Y. Imanishi, *J. Am. Chem. Soc.* **1997**, *119*, 1619.
[8] J. S. Mellors, J. W. Jorgenson, *Anal. Chem.* **2004**, *76*, 5441.
[9] M. Bedair, Z. El Rassi, *J. Chromatogr. A* **2005**, *1079*, 236.
[10] A. Barbetta, M. Massimi, L. C. Devirgiliis, M. Dentini, *Biomacromolecules* **2006**, *7*, 3059.
[11] M. Bokhari, R. J. Carnachan, S. A. Przyborski, N. R. Cameron, *J. Mater. Chem.* **2007**, *17*, 4088.
[12] E. Kjeang, R. Michel, D. A. Harrington, N. Djilali, D. Sinton, *J. Am. Chem. Soc.* **2008**, *130*, 4000.
[13] H. M. Simms, C. M. Brotherton, B. T. Good, R. H. Davis, K. S. Anseth, C. N. Bowman, *Lab Chip* **2005**, *5*, 151.
[14] X. Li, J. L. Coffer, Y. Chen, R. F. Pinizzotto, J. Newey, L. T. Canham, *J. Am. Chem. Soc.* **1998**, *120*, 11706.
[15] J. A. Burdick, D. Frankel, W. S. Dernell,K. S. Anseth, *Biomaterials* **2003**, *24*, 1613.
[16] P. Jiang, M. J. McFarland, *J. Am. Chem. Soc.* **2004**, *126*, 13778.

[17] H. Xu, X. Y. Ling, J. van Bennekom, X. Duan, M. J. W. Ludden, D. N. Reinhoudt, M. Wessling, R. G. H. Lammertink, J. Huskens, *J. Am. Chem. Soc.* **2009**, *131*, 797.
[18] J. Normatov, M. S. Silverstein, *Macromolecules* **2007**, *40*, 8329.
[19] A. Menner, R. Powell, A. Bismarck, *Soft Matter* **2006**, *2*, 337.
[20] C. Youssef, R. Backov, M. Treguer, M. Birot, H. Deleuze, *J. Polym. Sci. A* **2010**, *48*, 2942.
[21] U. H. F. Bunz, *Adv. Mater.* **2006**, *18*, 973.
[22] S. M. Gates, G. Dubois, E. T. Ryan, A. Grill, M. Lui, D. Gidley, *J. Electrochem. Soc.* **2009**, *156*, G156.
[23] D. O. H. Teare, W. C. E. Schofield, R. P. Garrod, J. P. S. Badyal, *Langmuir* **2005**, *21*, 10818.
[24] C. R. Savage, R. B. Timmons, J. W. Lin, *Chem. Mater.* **1991**, *3*, 575.
[25] M. E. Ryan, A. M. Hynes, J. P. S. Badyal, *Chem. Mater.* **1996**, *8*, 37.
[26] J. P. S. Badyal, *Chem. Br.* **2001**, *37*, 45.
[27] C. Tarducci, E. J. Kinmond, S. A. Brewer, C. Willis, J. P. S. Badyal, *Chem. Mater.* **2000**, *12*, 1884.
[28] L. G. Harris, W. C. E. Schofield, J. P. S. Badyal, *Chem. Mater.* **2007**, *19*, 1546.
[29] R. P. Garrod, L. G. Harris, W. C. E. Schofield, J. McGettrick, L. J. Ward, D. O. H. Teare, J. P. S. Badyal, *Langmuir* **2007**, *23*, 689.
[30] L. G. Harris, W. C. E. Schofield, K. J. Doores, B. G. Davis, J. P. S. Badyal, *J. Am. Chem. Soc.* **2009**, *131*, 7755.
[31] D. O. H. Teare, D. C. Barwick, W. C. E. Schofield, R. P. Garrod, L. J. Ward, J. P. S. Badyal, *Langmuir* **2005**, *21*, 11425.
[32] W. C. E. Schofield, J. McGettrick, T. J. Bradley, S. Przyborski, J. P. S. Badyal, *J. Am. Chem. Soc.* **2006**, *128*, 2280.
[33] D. O. H. Teare, W. C. E. Schofield, R. P. Garrod, J. P. S. Badyal, *J. Phys. Chem. B.* **2005**, *109*, 20923.
[34] W. C. E. Schofield, J. P. S. Badyal, *ACS Appl. Mater. Interfaces* **2009**, *1*, 2763.
[35] C. Tarducci, W. C. E. Schofield, S. A. Brewer, C. Willis, J. P. S. Badyal, *Chem. Mater.* **2002**, *14*, 2541.
[36] G. Øye, V. Roucoules, A. M. Cameron, L. J. Oates, N. R. Cameron, P. G. Steel, J. P. S. Badyal, B. G. Davis, D. Coe, R. Cox, *Langmuir* **2002**, *18*, 8996.
[37] K. Vasilev, L. Britcher, A. Casanal, H. J. Griesser, *J. Phys. Chem. B.* **2008**, *112*, 10915.
[38] M. Zelzer, M. R. Alexander, *J. Phys. Chem. B.* **2010**, *114*, 569.
[39] D. Lin-Vien, N. B. Colthup, W. G. Fateley, J. G. Grasselli, *The Handbook of Infrared and Raman Characteristic Frequencies of Organic Molecules*, Academic Press, Boston, USA **1991**.
[40] R. W. Horobin, *Histochemical J.* **1969**, *1*, 231.
[41] S. J. Isak, E. M. Eyring, *J. Photochem. Photobiol. A* **1992**, *64*, 343.
[42] E. Vogel, A. Gbureck, W. Kiefer, *J. Mol. Struct.* **2000**, *550–551*, 177.
[43] S. D. Kimmins, N. R. Cameron, *Adv. Funct. Mater.* **2011**, *21*, 211.
[44] A. Barbetta, N. R. Cameron, S. J. Cooper, *Chem. Commun.* **2000**, 221.
[45] Barbetta, A. M. Dentini, L. Leandri, G. Ferraris, A. Coletta, M. Bernabei, *React. Funct. Polym.* **2009**, *69*, 724.
[46] P. Hainey, I. M. Huxham, B. Rowatt, D. C. Sherrington, L. Tetley, *Macromolecules* **1991**, *24*, 117.
[47] A. Barbetta, N. R. Cameron, *Macromolecules* **2004**, *37*, 3188.
[48] S. Morsch, W. C. E. Schofield, J. P. S. Badyal, *Langmuir* **2010**, *26*, 12342.
[49] N. R. Cameron, *Polymer* **2005**, *46*, 1439.
[50] N. Shahidzadeh, D. Bonn, O. Aguerre-Chariol, J. Meunier, *Colloids Surf. A.* **1999**, *147*, 375.
[51] R. W. Greiner, D. F. Evans, *Langmuir* **1990**, *6*, 1793.
[52] P. Frederikson, T. Bjørnholm, H. G. Madsen, K. Bechgaard, *J. Mater. Chem.* **1994**, *4*, 675.
[53] Y. Uda, F. Kaneko, N. Tanigaki, T. Kawaguchi, *Adv. Mater.* **2005**, *17*, 1846.
[54] C. Larpent, E. Bernard, J. Richard, S. Vaslin, *React. Funct. Polym.* **1997**, *33*, 49.
[55] C. Larpent, E. Bernard, J. Richard, S. Vaslin, *Macromolecules* **1997**, *30*, 354.
[56] J. R. Becker, *Crude Oil Waxes, Emulsions and Asphaltenes*, PennWell Books, Tulsa, USA **1997**.
[57] S. D. Alexandratos, X. Zhu, *Macromolecules* **2003**, *36*, 3436.
[58] I. Gurevitch, M. S. Silverstein, *J. Polymer Sci. A* **2010**, *48*, 1516.
[59] A. K. Das, D. Mukesh, V. Swayambunathan, D. D. Kotkar, P. K. Ghosh, *Langmuir* **1992**, *8*, 2427.
[60] A. Ram, *Fundamentals of Polymer Engineering* Plenum Press New York, **1997**.
[61] S. A. Baeurle, A. Hotta, A. A. Gusev, *Polymer* **2006**, *47*, 6243.
[62] R. J. Carnachan, M. Bokhari, S. A. Przyborski, N. R. Cameron, *Soft Matter* **2006**, *2*, 608.
[63] S. Zhang, J. Chen, V. T. Perchyonok, *Polymer* **2009**, *50*, 1723.
[64] J. Eastoe, B. H. Robinson, D. C. Steytler, *J. Chem. Soc. Faraday Trans.* **1990**, *86*, 511.
[65] J. M. Williams, A. J. Gray, M. H. Wilkerson, *Langmuir* **1990**, *6*, 437.
[66] D. Bontempo, H. D. Maynard, *J. Am. Chem. Soc.* **2005**, *127*, 6508.
[67] F. J. Xu, L. Y. Liu, W. T. Yang, E. T. Kang, K. G. Neoh, *Biomacromolecules* **2009**, *10*, 1665.
[68] C. D. Ehrlich, J. A. Basford, *J. Vac. Sci. Technol. A.* **1992**, *10*, 1.
[69] D. Lovering, *NKD-6000 Technical Manual*, Aquila Instruments, Cambridge UK **1998**.